ISSN 1330-3651 (Print), ISSN 1848-6339 (Online)
DOI: 10.17559/TV-20141207160855

DISTRIBUTION CHARACTERISTICS ANALYSIS OF PRESSURE-ARCH IN HORIZONTAL STRATIFIED ROCKS UNDER COAL MINING CONDITIONS

Shu-ren Wang, Ning Li, Chun-liu Li, Chen Cao

Original scientific paper
The criteria of separation and dislocation of the layered roof in mining are put forward through the simplified mechanical model with weak inter-layers. Considering five different variables, namely the number of layers, the distance from the weak inter-layers to the mine opening, the thickness of the weak inter-layers, the lateral pressure coefficient and the spacing of the bedding planes, the distribution characteristics of the pressure-arch in the horizontal stratified rocks are analyzed during coal mining using FLAC3D. The results show that the newly appeared pressure-arch is composed of the original pressure-arch in each layer and the pressure-arch shape being affected by the weak layer in the surrounding rock of the mine opening. As the distance between the inter-layers and the coal seam increases, the effect on the pressure-arch is reduced gradually. The thinner inter-layers produce greater impact on the pressure-arch. The lateral pressure coefficient has a great influence on the pressure-arch and a stable pressure-arch could only be formed when the lateral pressure coefficient is in a suitable range.

Keywords: *numerical analysis; pressure-arch; stratified rock; weak inter-layers*

Analiza karakteristika raspodjele tlaka stropa u horizontalno slojevitim stijenama u uvjetima iskapanja ugljena

Izvorni znanstveni članak
Predlažu se kriteriji za odvajanje i premještanje slojevitog nadsvođa u rudarstvu primjenom pojednostavljenog mehaničkog modela sa slabim međuslojevima. Uz razmatranje pet različitih varijabli, naime broja slojeva, razmaka od slabih među-slojeva do otvora rudnika, debljine slabih međuslojeva, lateralnog koeficijenta tlaka i međusobnog razmaka površina laminacije, analiziraju se karakteristike raspodjele tlaka stropa u horizontalno slojevitim stijenama tijekom iskapanja ugljena, primjenom FLAC3D. Rezultati pokazuju da se novonastali tlak stropa sastoji od originalnog tlaka stropa u svakom sloju te tlaka konture stropa prouzročenog slabim slojem u okruženju stijene okna rudnika. Kako se povećava razmak između međuslojeva i sloja (žile) ugljena, postepeno se smanjuje utjecaj na tlak stropa. Tanji međuslojevi imaju veći utjecaj na tlak stropa. Lateralni koeficijent tlaka ima veliki utjecaj na tlak stropa te se stabilni tlak stropa može stvoriti jedino kad je lateralni koeficijent tlaka odgovarajućeg raspona.

Ključne riječi: *numerička analiza; slabi međuslojevi; slojevita stijena; tlak stropa*

1 Introduction

The pressure-arch of the mine opening is the result of the redistribution of stress, which both promotes the stability and reflects the strength of the surrounding rock [1 ÷ 4]. The surrounding rock of coal excavation is composed of the stratified rocks including primary structural planes, such as the bedding and also the weak inter-layers. The physical and mechanical characteristics of the stratified rocks are transverse isotropic and orthogonal anisotropic materials largely due to the weak inter-layers [5 ÷ 7]. These structural planes will affect the shape and the extent of the pressure-arch and the stability of the surrounding rock. Therefore, it is of great significance to investigate the distribution characteristics of the pressure-arch in the horizontal stratified rocks.

In recent years, many scholars have conducted relevant research on the stratified rocks or on the surrounding rock with weak inter-layers using many methodologies, including field investigation, numerical simulations, physical model tests and analytical analyses. For example, Zhang et al. revealed the destruction and instability mechanism of the rock mass with weak inter-layers through mechanical analysis [8]. Jia et al. studied the failure mechanism of the stratified rock roof of the tunnel [9]. When a layered system of rock beds is subjected to a sufficiently large extensional strain, joints form in the competent layers. Jain et al. found that the joint spacing first decreases and then increases with depth for a given applied strain [10]. Zhang et al. discussed the weak inter-layers with different distances that affected the stability of the underground cavern [11]. Yang et al. studied the deformation and failure of the stratified rocks under different supporting schemes and proposed reasonable supporting parameters [12]. Fortsakis et al. explored the anisotropic behaviour of the stratified rocks and analyzed the effects on the structural planes with different dip angles [13]. Wang et al. found that not only the depth of the tunnel, but also the parameters of the joints had significant effects on the loose zone in the stratified rocks [14]. Hrestak et al. analysed the distribution of stresses and strains during the portal section excavation for the right tube of the Sleme Tunnel by the Finite Element Method (FEM). The results verified that for this particular case a sufficiently safe and cost-efficient construction technology was applied [15]. Li et al. researched the effects of thin coal seam on the roof of roadways with different thicknesses and positions. They found the deformation and failure mechanism of the surrounding rock to the corresponding supporting measures of the roadway [16].

In summary, these studies have reached some important conclusions regarding the instability mechanisms of the stratified rocks. However, these studies of failure characteristics of the stratified rocks are not sufficiently detailed and the research on the pressure-arch in the stratified rocks during coal mining is also lacking. Therefore, it is of significance to study the pressure-arch distribution characteristics in the horizontal stratified rocks for coal mining and tunnels supporting.

2 Forming mechanism of pressure-arch in the stratified rocks

As shown in Fig. 1, with underground coal being mined-out, three distinct zones gradually form in the overlying rock of after the mine excavation: the stress-

relief zone, the pressure-arch zone and the original-rock zone. The horizontal stratified rock containing the weak inter-layers can be simplified as a layered structure model as illustrated in Fig. 1.

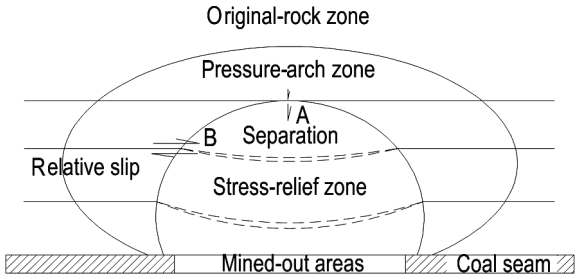

Figure 1 Pressure-arch in stratified rocks after coal being mined-out

In the layered structure model, the mechanical condition of the adjacent strata, which has produced relative dislocation at point A, can be described as follows:

$$\tau > c + \sigma \cdot \tan\varphi \tag{1}$$

where τ is the shear stress, σ is the normal stress, c is the cohesion and φ is the internal friction angle of the adjacent layers at point A.

For the adjacent strata to separate at point B, it should meet all three of the following conditions:

(a) The lithology of the upper part is harder than that of the lower part.

$$f_{\text{upper}} > f_{\text{lower}} \tag{2}$$

where f_{upper} and f_{lower} are the hardness in the protodrakonov scale of the upper and lower parts at point B respectively.

(b) The mechanical condition is that the shear stress exceeds the shear strength of the layers at point B, or:

$$\sigma > \sigma_{\text{t}} \tag{3}$$

where σ is the normal stress and σ_{t} is the tensile strength of the adjacent layers at point B.

(c) The deformation condition is given as follows:

$$W_{\text{upper}} > W_{\text{lower}} \tag{4}$$

where W_{upper} and W_{lower} are the vertical deflection of the upper and lower parts at point B respectively.

After the coal is mined out, due to lack of rock support, the separation occurs in the overlying rock in the mine opening and the relative slip between layers appears. The deformation and the damage in the stratified rocks result in a stress-relief zone being formed. From the stress-relief zone to the deep rock in the mine opening, the deformation gradually reduces whereas the stress gradually increases until the peak is reached. From the pressure-arch zone to the deeper surrounding rock, the stress gradually returns to the initial state to form a transition zone before reaching the original-rock zone.

3 Computational model and mechanical characteristics of the pressure-arch

3.1 The computational model

As shown in Fig. 2, the three-dimensional computational model was built using FLAC^{3D} under the fully-mechanized mining conditions. The computational model is 240 m long, 240 m wide and 200 m high, and the dimensions of the fully-mechanized mining panel are 100 m long, 100 m wide and 3,5 m high in the *X*-, *Y*-, and *Z*-axis, respectively. There is a 600 m thick rock mass above the top of the model with the average density of 2500 kg/m^3, which can be converted into an application of a vertical load of p on the model, i.e., p = 15 MPa.

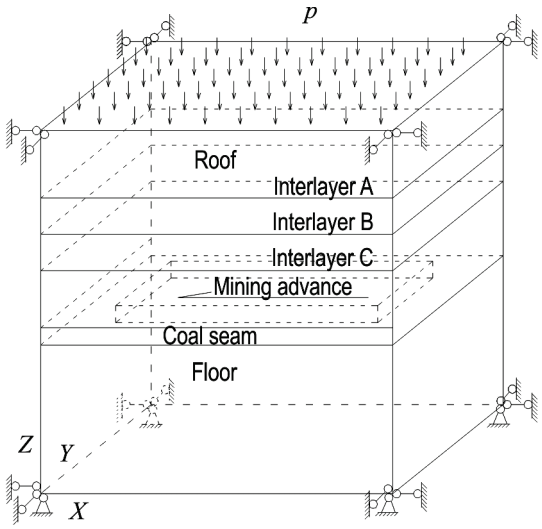

a) Three-dimension model

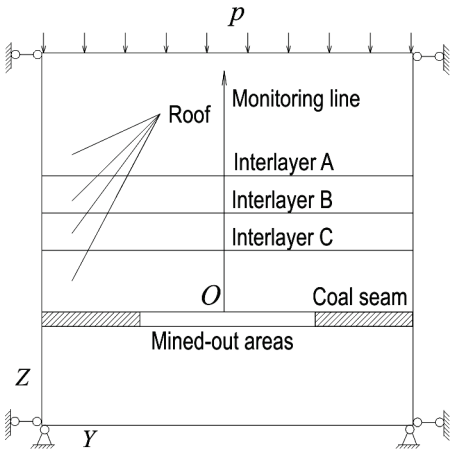

b) Y-Z section of the model

Figure 2 Schematic of the computational model

The horizontal displacement of the four lateral boundaries of the model was restricted, the vertical load p was applied onto the top of the model, and its bottom was fixed. The material of the model was supposed to meet the Mohr-Coulomb strength criterion, and the physical and mechanical parameters were selected and listed in Tab. 1.

3.2 Mechanical characteristics of the pressure-arch

Based on previous research results [4], the inner boundary of the pressure-arch was fixed at the peak point

of maximum principal stress and its outer boundary was fixed at the point where the ratio of maximum principal stress to the difference between the maximum principal stress and the minimum principal stress was equal to 10 %.

Table 1 Physical and mechanical parameters of the model

Name	Den. (kg/m^3)	Ela. (GPa)	Poission's ratio	Ten. (MPa)	Coh. (MPa)	Fri. (°)
Layer 1	2600	8,0	0,36	1,2	4,0	36
Layer 2	2600	11,0	0,33	1,5	4,5	38
Layer 3	2600	14,0	0,30	1,7	5,0	40
Layer 4	2600	17,0	0,28	2,0	8,0	43
Roof	2600	23,0	0,24	2,5	9,0	44
Coal seam	1440	3,0	0,38	1,0	3,0	30
Floor	2700	25,0	0,23	3,0	10,0	45
Bedding	-	-	-	0,1	0,3	24
Weak inter-layers	2550	2,0	0,40	0,1	0,3	24

As shown in Figs. 2 and 3, along the positive direction on the *Z*-axis along the monitroing line, the greater the vertical distance *H* between the overlying strata and the coal seam, the lesser the vertical displacement. In addition, as *H* increases, both the maximum and the minimum principal stress gradually rise. At the position of the structural plane, the maximum principal stress reduces and delamination occurs.

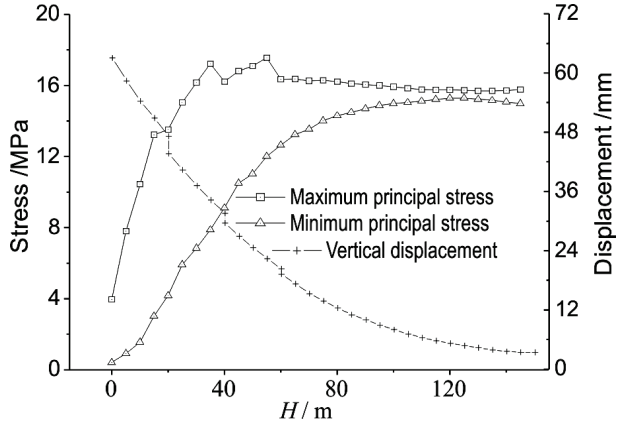

Figure 3 Stress and vertical displacement on the *Y-Z* section

When *H* reaches at 55 m along the monitoring line, the maximum principal stress reaches the peak value and separation no longer occurs at the inner boundary of the pressure-arch. Similarly, when *H* reaches at 100 m, the ratio of the maximum principal stress to the difference between the maximum and the minimum principal stress is equal to 10 %, i.e., the stress gradually returns to the initial state, where the outer boundary of the pressure-arch is determined.

As shown in Figs. 2 and 4, along the positive direction on the *Y*-axis, the displacements are different. This means that relative slip appears at inter-layers B. The relative slip reaches the maximum value at the points of 72,5 m and 167,5 m, and the tendencies of shear stress and shear displacement are similar. Thus the inner boundary of the pressure-arch could be determined at the point where the shear stress reached maximum value. Relative slip reaches the minimum value at the points of 42,5 m and 197,5 m, and the shear stress gradually returns to the initial state; here the outer boundary of the pressure-arch could be determined.

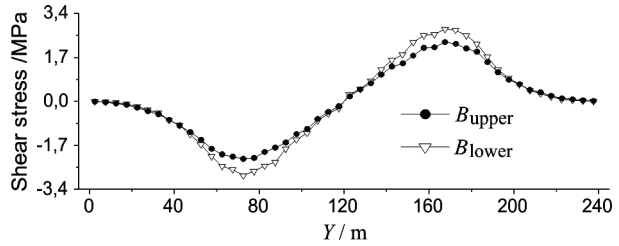

a) Shear stress on inter-layers B

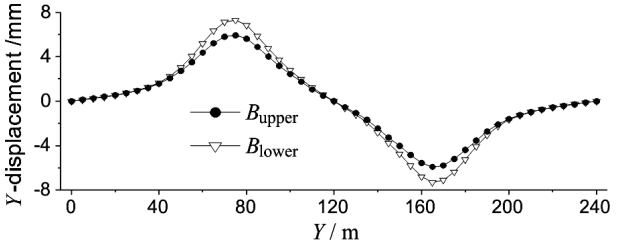

b) *Y*-displacement curves

Figure 4 Shear stress on inter-layers B and *Y*-displacement curves.

3.3 Numerical simulation programs

In order to reflect the distribution characteristics of the pressure-arch in horizontal stratified rocks under different conditions, five calculation projects were formulated and listed in Tab. 2.

Table 2 Calculation projects of the computational model

Project	Variable	Value
1	Number of inter-layerss (*N*)	0, 1, and 3
2	Distance from the weak inter-layers to the coal seam (*H*)	30 m, 80 m, and 120 m
3	Thickness of the weak inter-layers (*T*)	0,01 m, 0,5 m and 1,0 m
4	Lateral pressure coefficient (λ)	0,95, 1,0 and 1,2
5	Spacing of the bedding plane (*S*)	10 m, 20 m and 30 m

4 Result and discussion

4.1 Variation of the number *N* of inter-layers

As shown in Fig. 5a, without stratification of the surrounding rock, the shape of the pressure-arch in the fully-mechanized mining field is symmetrical and its boundaries form a smooth curve. Fig. 5b shows that when there is one weak inter-layer in the surrounding rock, the pressure-arch formed in the upper and lower parts constitutes a new pressure-arch. The thickness and height of the new pressure-arch are higher, and it becomes flat at the vault. The outer boundary of the new pressure-arch at the weak inter-layers moves inward, forming a dent. In Fig. 5c, when there are three inter-layers in the surrounding rock with 20 m spacing, the change in the shape of the pressure-arch is more apparent. The new pressure-arch becomes pointed at the vault. The inner and outer boundaries of the pressure-arch move inward and obvious faulting results in the structural planes. As seen from Fig. 5c, the degree of faulting tends to a more significant extent with the inter-layers closer to the vault of the pressure-arch. The inner boundary at the vault is limited between the first and the second planes.

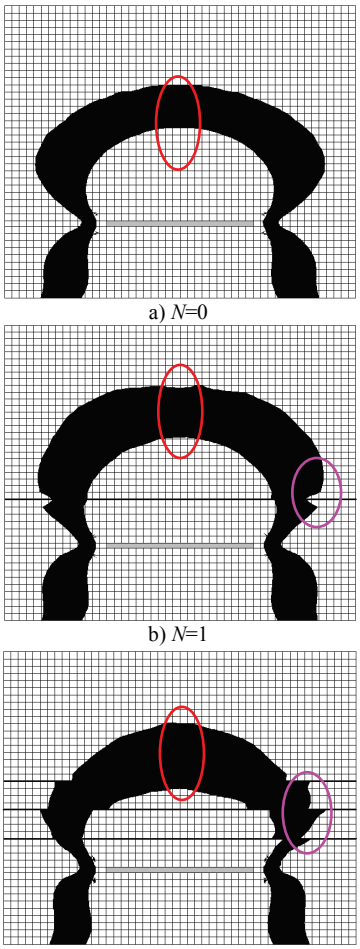

a) N=0

b) N=1

c) N=3

Figure 5 Shape of pressure-arch variation of N

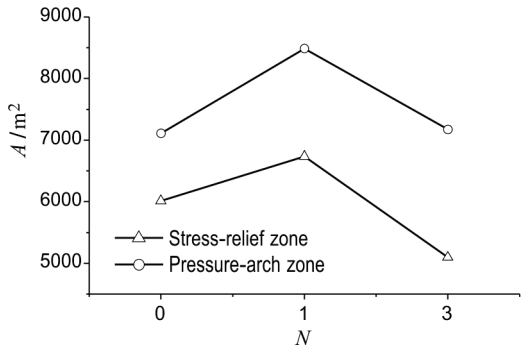

a) Zone areas A variation of N

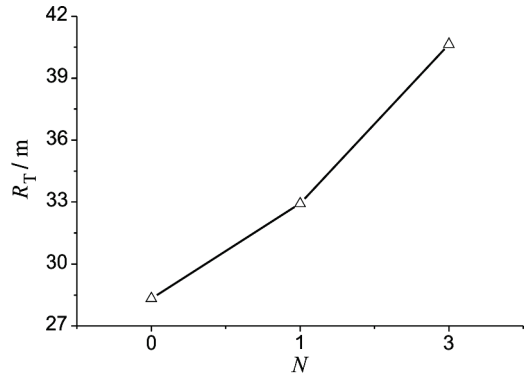

b) Vault thickness R_T variation of N

Figure 6 Zone areas A and vault thickness R_T variation of N

As shown in Fig. 6a, when there was one weak inter-layer in the surrounding rock, both areas A of stress-relief and pressure-arch zones are larger than the other two values and the area of pressure-arch zone is larger than that of the stress-relief. In Fig. 6b, the thickness R_T of the vault of the pressure-arch tends to increase with the increase of number of inter-layers N. It can be seen that the inter-layers could change the shape and distribution of the pressure-arch, therefore affecting its formation. The shear failures are easier to produce in the structural planes.

4.2 Variation of the distance H from the weak inter-layer to the coal seam

The distance between the weak inter-layer and the coal seam also affects the pressure-arch. As shown in Fig. 7a, when H is 30 m, the thickness of the pressure-arch is the greatest and the outer boundary of the pressure-arch spreads to the deeper rock. In Fig. 7b, when H is 80 m, the weak inter-layers have no effect on the inner boundary of the pressure-arch, but make the outer boundary move inward. Fig. 7c shows that when H is 120 m, the weak inter-layer has no effect on the pressure-arch. Seen from Fig. 8, the vault thickness R_T of the pressure-arch and the areas A of the stress-relief and pressure-arch zones nearly both decrease with the increase of the distance H from the weak inter-layer to the coal seam. It can be concluded that the weak inter-layer almost affects the pressure-arch when the pressure-arch is above the weak inter-layer.

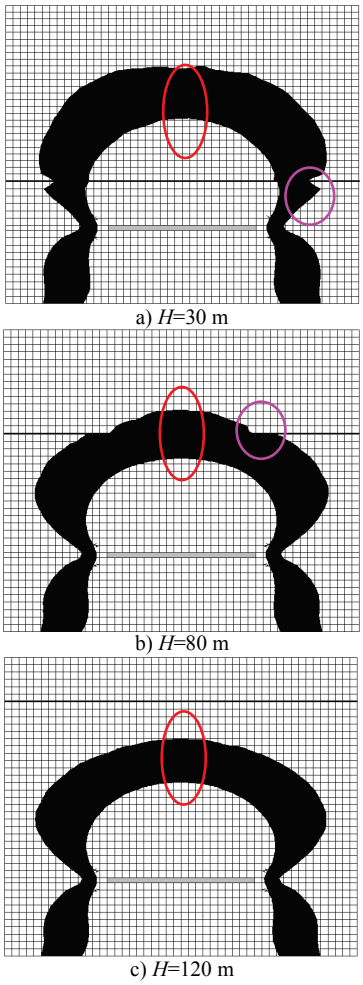

a) H=30 m

b) H=80 m

c) H=120 m

Figure 7 Shape of pressure-arch variation of H

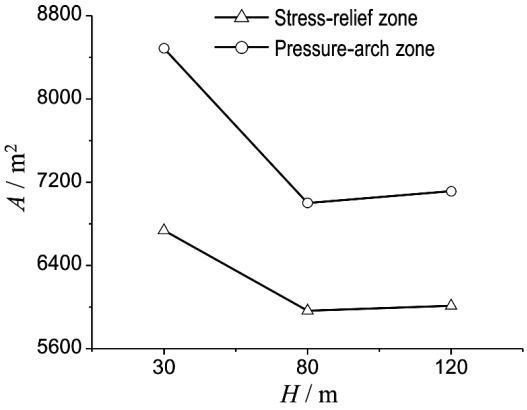

a) Zone areas A variation of H

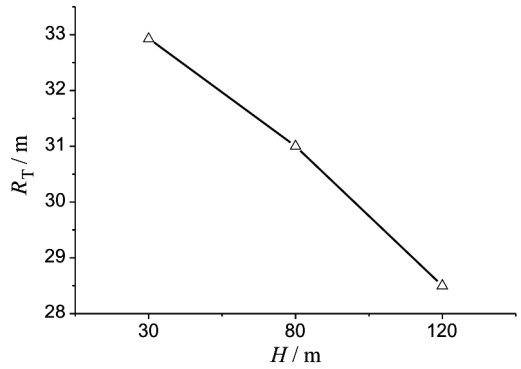

b) Vault thickness R_T variation of H

Figure 8 Zone areas A and vault thickness R_T variation of H

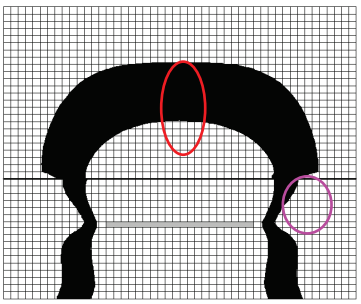

a) T=0,01 m

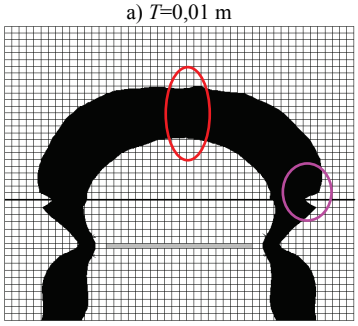

b) T= 0,5 m

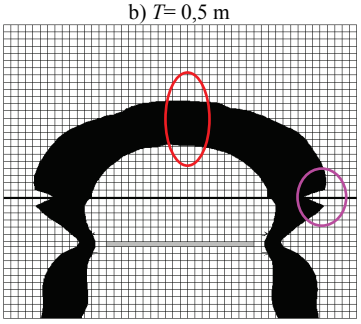

c) T=1,0 m

Figure 9 Shape of pressure-arch variation of T

4.3 Variation of the thickness *T* of the weak inter-layer

As shown in Fig. 9, as the thickness of the weak inter-layer rises, the thickness and the height of the pressure-arch above the weak inter-layer reduce. This means that a thinner weak inter-layer has a negative effect on the carrying capacity of the pressure-arch and more rocks are needed to participate in the transmission of load. As seen from Fig. 10, not only the vault thickness R_T of the pressure-arch, but also the areas A of the stress-relief and pressure-arch zones totally decrease with the thickness T increase of the weak inter-layer. However, the thickness of the pressure-arch with the weak inter-layer increases, which results in the formation of several larger dents on the pressure-arch.

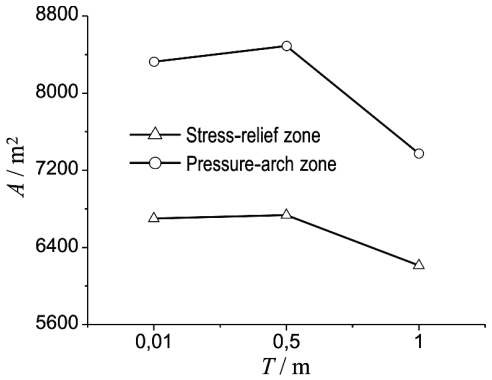

a) Zone areas A variation of T

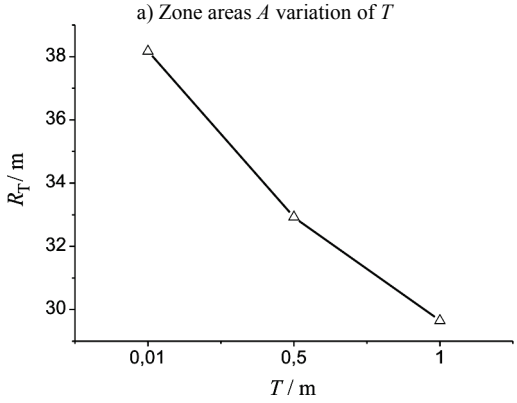

b) Vault thickness R_T variation of T

Figure 10 Zone areas A and vault thickness R_T variation of T

4.4 Variation of the lateral pressure coefficient

As shown in Fig. 11, as the lateral pressure coefficient λ increases, the height of the pressure-arch increases significantly. The thickness of the vault increases but that of the feet reduces. The shape of the pressure-arch changes gradually from a flat arch to a cuspate arch as the lateral pressure coefficient changes from $\lambda < 1$ to $\lambda > 1$. In Fig. 12, with λ changing from 0,95, 1,0 to 1,2, both the areas A of the stress-relief zones and the vault thickness R_T of the pressure-arch increase significantly. However, the area A of the pressure-arch zone first increases then reduces with that of λ increase. If the lateral pressure coefficient is too small, there is no pressure-arch being formed. Conversely, if the lateral pressure coefficient is too large, no pressure-arch is followed on the sides of the mine excavation. So, a stable pressure-arch could form only when the lateral pressure coefficient is appropriate.

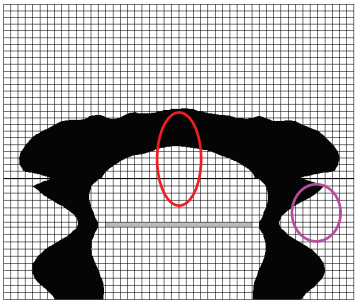

a) λ=0,95

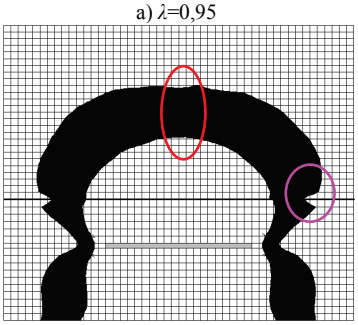

b) λ=1,0

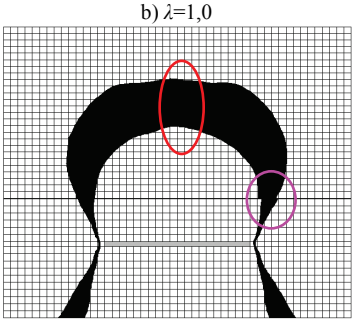

c) λ=1,2

Figure 11 Shape of pressure-arch variation of λ

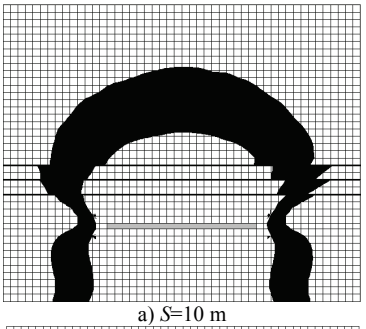

a) S=10 m

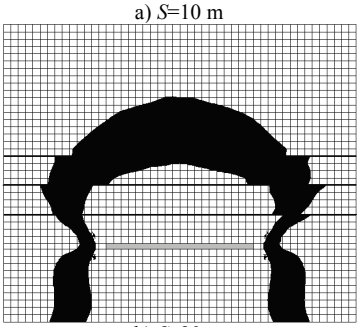

b) S=20 m

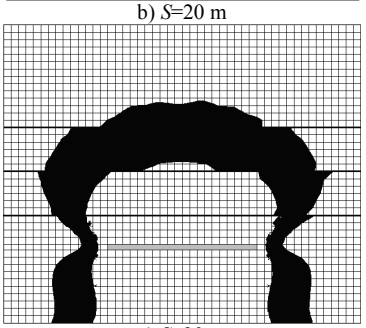

c) S=30 m

Figure 13 Shape of pressure-arch variation of S

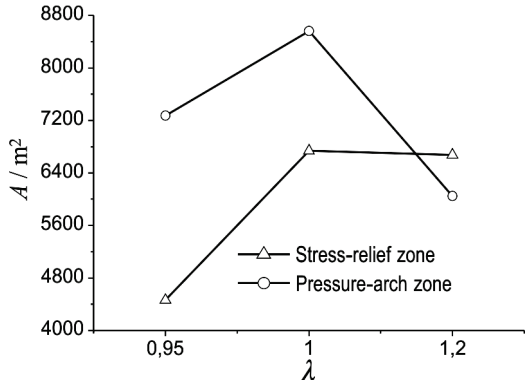

a) Zone areas A variation of λ

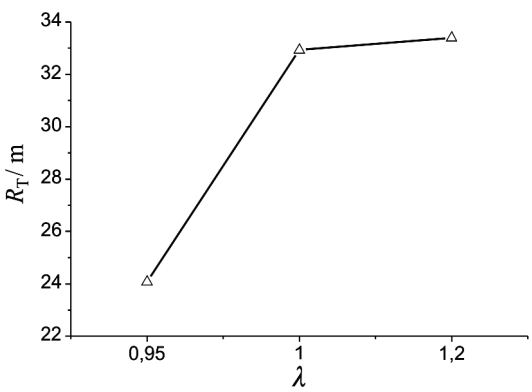

b) Vault thickness R_T variation of λ

Figure 12 Zone areas A and vault thickness R_T variation of λ

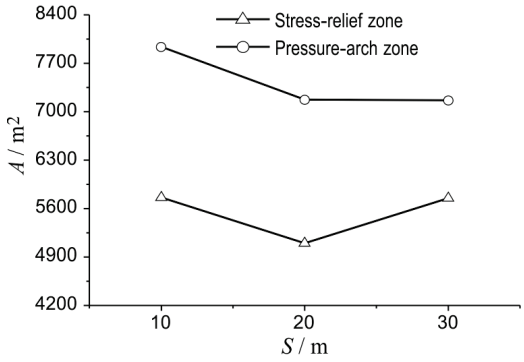

a) Zone areas A variation of S

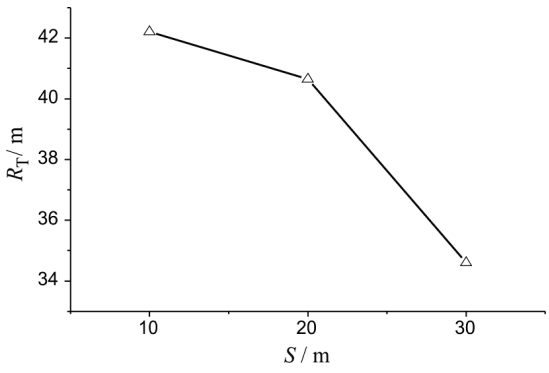

b) Vault thickness R_T variation of S

Figure 14 Zone areas A and vault thickness R_T variation of S

4.5 Variation of the spacing *S* of the bedding plane

As shown in Fig. 13, when the spacing is 10 m, tangential dislocations appear in the pressure-arches in every layer. Compared with the spacings of 10 m, 20 m and 30 m, the faulting effects are abated as the spacing becomes larger, and the pressure-arch retracts to being thin and flat. In Fig. 14, as *S* changes from 10 m, 20 m to 30 m, the areas *A* of pressure-arch zone and the vault thickness of the pressure-arch all reduce obviously. The areas *A* of stress-relief zone first decrease then increase with increasing *S*. The results show that structural planes would reduce the bearing capacity of the surrounding rock and more rocks are needed to bear the loads.

5 Conclusions

Compared to the surrounding rock without a weak inter-layer, the new forming pressure-arch in the stratified rock appears indented at the primary structural planes. Those structural planes limit the development of the pressure-arch and reduce the stability of the surrounding rock.

The weak inter-layers influence the pressure-arch when the pressure-arch is above the weak inter-layers, and these effects would reduce as the distance between the weak inter-layers and the coal seam increase. The thickness of the weak inter-layers has an impact on the shape of the pressure-arch.

Furthermore, as the lateral pressure coefficient increases, the height of the pressure-arch increases significantly and the shape changes from a flat arch to a cuspate arch. A stable pressure-arch can form only when the lateral pressure coefficient is appropriate. The spacing of the structural plane affects the distribution of the pressure-arch and the smaller spacing is more disadvantageous in terms of the bearing capacity of the surrounding rock.

Acknowledgments

This work was financially supported by the National Natural Science Foundation of China (Nos. 51474188; 51074140; 51310105020), the Natural Science Foundation of Hebei Province of China (E2014203012), 2015 Endeavor Research Fellowship and Program for Taihang Scholars, all these are gratefully acknowledged.

6 References

[1] Poulsen, B. A. Coal pillar load calculation by pressure arch theory and near field extraction ratio. // International Journal of Rock Mechanics and Mining Sciences. 47, 7(2010), pp. 1158-1165. DOI: 10.1016/j.ijrmms.2010.06.011

[2] Wang, S. R.; Hagan, P.; Cheng, Y.; Wang, H. Experimental research on fracture hinged arching process and instability characteristics for rock plates. // Chinese Journal of Rock Mechanics and Engineering. 31, 8(2012), pp. 1674-1679.

[3] Wu, Y. P.; Wang, H. W.; Xie, P. S. Analysis of surrounding rock macro-stress arch-shell of long-wall face in steeply dipping seam mining. // Journal of China Coal Society. 37, 4(2012), pp. 559-564.

[4] Wang, S. R.; Li, N.; Li, C. L.; Hagan, P. Mechanics evolution characteristics analysis of pressure-arch in fully-mechanized mining field. // Journal of Engineering Science and Technology Review, 7, 4(2014), pp. 40-45.

[5] Li, G. R.; She, C. X.; Chen, S. H. Destructive testing and finite element analysis of bending deformation of layered rock slope. // Chinese Journal of Rock Mechanics and Engineering. 16, 4(1997), pp. 305-311.

[6] Wang, S. R.; Xu, D. F.; Hagan, P.; Li, C. L. Fracture characteristics analysis of double-layer rock plates with both ends fixed condition. // Journal of Engineering Science and Technology Review. 7, 2(2014), pp. 60-65.

[7] Wang, S. R.; Wang, Z. Q. Analysis of separation and dislocation characteristics of layered roof in the mined-out areas. // Applied Mechanics and Materials. 256-259, (2013), pp. 75-80. DOI: 10.4028/www.scientific.net/AMM.256-259.75

[8] Zhang, D. L; Wang, H. Y.; Qu, T. Z. Influence analysis of interface on stability stratified rock mass. // Chinese Journal of Rock Mechanics and Engineering. 19, 2(2000), pp. 140-144.

[9] Jia, P.; Tang, C. A.; Wang, S. H. Destroy mechanism of tunnel with stratified roof. // Journal of China Coal Society. 31, 1(2006), pp. 11-15.

[10] Jain, A.; Guzina, B. B.; Voller, V. R. Effects of overburden on joint spacing in layered rocks. // Journal of Structural Geology. 29, (2007), pp. 288-297. DOI: 10.1016/j.jsg.2006.08.010

[11] Zhang, Z. P.; Li, N.; Chen, F. F.; Swoboda, G. Influence of different distance of weak interface on stability of underground openings. // Rock and Soil Mechanics. 28, 7(2007), pp. 1363-1368.

[12] Yang, J. P.; Chen, W. Z.; Zheng, X. H. Stability study of deep soft rock roadways with weak intercalated layers. // Rock and Soil Mechanics. 29, 10(2008), pp. 2864-2870.

[13] Fortsakis, P.; Nikas, K.; Marinos, V.; Marinos, P. Anisotropic behaviour of stratified rock masses in tunneling. // Engineering Geology. 141-142, (2012), pp. 74-83. DOI: 10.1016/j.enggeo.2012.05.001

[14] Wang, Z. W.; Qiao, C. S.; Song, C. Y.; Xu, J. F. Upper bound limit analysis of support pressures of shallow tunnels in layered jointed rock strata. // Tunneling and Underground Space Technology. 43, (2014), pp. 171-183. DOI: 10.1016/j.tust.2014.05.010

[15] Hrestak, T.; Jaguljnjak Lazarević, A.; Frgić, L. Stress and strain analysis during the Sleme tunnel excavation. // Tehnički vjesnik-Technical Gazette. 22, 3(2015), pp. 703-709. DOI: 10.17559/TV-20140530103847

[16] Li, W. T.; Wang, Q.; Li, S. C.; Wang, D. C.; Huang, F. C.; Zuo, J. Z.; Zhang, S. G.; Wang, H. T. Deformation and failure mechanism analysis and control of deep roadway with intercalated coal seam in roof. // Journal of China Coal Society. 39, 1(2014), pp. 47-56.

Authors' addresses

Shu-ren Wang, Ph.D., Professor, *Corresponding author*
1) Opening Laboratory for Deep Mine Construction, Henan Polytechnic University, 2001 Century Avenue, Jiaozuo, Henan Province, 454003, China

2) School of Civil Engineering and Mechanics, Yanshan University No. 438 Hebei West Street, Haigang District, Qinhuangdao, 066004, China, E-mail: w_sr88@163.com

Ning Li, postgraduate
School of Civil Engineering and Mechanics, Yanshan University No. 438 Hebei West Street, Haigang District, Qinhuangdao, 066004, China, E-mail: j376131745@163.com

Chun-liu Li, postgraduate
1) School of Civil Engineering and Mechanics, Yanshan University No. 438 Hebei West Street, Haigang District, Qinhuangdao, 066004, China

2) Institute of Urban Construction, Hebei Normal University of Science & Technology, No. 360 Hebei West Street, Haigang District, Qinhuangdao, 066004, China
E-mail: lclcc_010@163.com

Chen Cao, Ph.D.
Engineering Faculty, University of Wollongong
Engineering Faculty, University of Wollongong, NSW 2530, Australia, E-mail: ccao@uow.edu.au